2016-01-1161

Comparison of RCCI Operation with and without EGR over the Full Operating Map of a Heavy-Duty Diesel Engine

Author, co-author (Do NOT enter this information. It will be pulled from participant tab in MyTechZone)

Affiliation (Do NOT enter this information. It will be pulled from participant tab in MyTechZone)

Abstract

Dual-fuel combustion using port-injection of low reactivity fuel combined with direct injection of a higher reactivity fuel, otherwise known as Reactivity Controlled Compression Ignition (RCCI), has been shown as a method to achieve low-temperature combustion with moderate peak pressure rise rates, low engine-out soot and NO_x emissions, and high indicated thermal efficiency. A key requirement for extending to high-load operation is moderating the reactivity of the premixed charge prior to the diesel injection. One way to accomplish this is to use a very low reactivity fuel such as natural gas. In this work, experimental testing was conducted on a 13L multi-cylinder heavy-duty diesel engine modified to operate using RCCI combustion with port injection of natural gas and direct injection of diesel fuel.

Natural gas/diesel RCCI engine operation is compared over the EPA Heavy-Duty 13 mode supplemental emissions test with and without EGR. Emissions and efficiency metrics were examined over the full load engine map for both operating modes. It was found that the use of light EGR lowered cycle averaged NO_x emissions by 48%, with only a slight increase in soot and 0.5 point decrease in brake thermal efficiency, thus offering the lowest total fluid consumption when considering the use of a selective catalytic reduction system for NO_x aftertreatment.

Introduction

Strict new standards for CO_2 emissions and fuel consumption of heavy-duty engines and vehicles [1], coupled with the business interests of heavy-duty vehicle operators to reduce total cost of ownership, drive an increased push for high-efficiency heavy-duty motive power. Stringent emissions standards also mandate low system-out (including engine and aftertreatment) levels of gaseous (including NO_x and NMHC) and particulate emissions [2]. Reflecting the need for higher efficiency heavy-duty engines, key objectives of the Department of Energy (DOE) SuperTruck program include the demonstration of a heavy-duty engine with 50% brake thermal efficiency and establishment of a pathway to 55% brake thermal efficiency [3]. Many previously developed low-temperature diesel combustion strategies produce low engine-out emissions but frequently at the penalty of lower engine efficiency. However, increasingly effective aftertreatment systems for heavy-duty diesel engines have enabled higher overall engine efficiency [4] – combustion concepts designed to produce low engine-out emissions must therefore also deliver comparable efficiencies to remain competitive. Dual-fuel combustion concepts were developed as a method of addressing the limitations of earlier low-temperature combustion strategies while providing high engine efficiency.

By introducing two fuels of differing reactivity into the combustion chamber separately, overall fuel reactivity levels can be adjusted with operating conditions. Further, separating the fuel delivery, port-injecting the low reactivity fuel and direct injecting the high reactivity fuel, has been shown to create in-cylinder reactivity stratification, slowing combustion and decreasing the pressure rise rate, a primary load-limiting factor for many HCCI-type combustion strategies [5,6]. Dual-fuel strategies using gasoline and diesel have shown potential for high efficiency, both quantified by indicated thermal efficiency measurements on single-cylinder engines [5,6] and by brake thermal efficiency measurements on multi-cylinder engines [7,8,9]. By using a low compression ratio, it has been shown that a dual-fuel concept can cover the entire operating range of a heavy-duty engine [10]; efficiency with the low compression ratio, however, may not offer advantages over current single-fuel conventional diesel engines.

Different variations on the dual-fuel concept have been explored, with key differences being the delivery conditions of the diesel injection. The Reactivity Controlled Compression Ignition (RCCI) concept uses very early injection timing with relatively low injection pressure – start of combustion and subsequent combustion phasing is largely kinetically driven [5,6]. A similar concept has also been reported in literature [8,11,12]. However, by using a more conventionally timed, high pressure, single diesel injection, greater control over the combustion phasing can be achieved and, depending on the thermal boundary conditions, potentially an expansion of the upper load limit of the operating range can be accomplished [7,8,9].

Despite all of the work on kinetically controlled RCCI, it has been typically limited to the low to mid load range. Thus, there is still a need to reach full load, i.e. 20+ bar BMEP. Recent work [13-17] has looked at combining both kinetically and mixing controlled combustion strategies as a method to

increase the peak load capability of advanced combustion modes. Such strategies, called Adaptive Injection Strategies (AIS), have used a mixed mode or even a two stage combustion strategy where a fraction of the fuel is injected early for premixed auto-ignition combustion followed by a late, mixing controlled combustion event to reach the target load without increasing the maximum pressure rise rate (MPRR). Practically, methods to achieve this have been to use either two fuels and two direct injections or one fuel and two direct injectors [13-17]. In these two modes, results (at mid load conditions) achieved low NO_x and reasonable efficiencies, but could have excessive soot, which was very sensitive to the cylinder conditions at the SOI, namely the temperature and O_2 concentration. The goals for this work are to improve on these past results by using two fuels with PFI and a single direct injection in order to realize full load operation with RCCI.

Experimental Configuration

Low speed measurements of engine operating parameters, including temperatures, pressures, emissions, and fuel flow are logged at 10 Hz. High speed combustion data were taken using commercially available software, which was also used to post process the pressure data.

Crank-angle resolved measurements of cylinder pressure are collected using Kistler 6125B transducers in all six cylinders at 0.1 crank angle degree resolution for 300 engine cycles. A 3 kHz low-pass filter is used to suppress significant cylinder pressure oscillation due to chamber resonance. In all the results, pressure data from cylinder number 2 were chosen as the most representative cylinder of the overall engine operation.

Gaseous emissions are measured using a standard 5-gas analyzer (Horiba MEXA-7100DEGR), which includes CO_2 measurements in the intake for EGR calculation and a second FID for dedicated CH_4 emissions measurements. An AVL 415 Smoke Meter is used for soot emissions measurements.

Fuel flow rates, for both natural gas and diesel fuel, are measured with Micro Motion CMFS010 Coriolis-type flowmeters. The airflow rate was measured using a laminar flow element.

The test engine used in this study is a MY2010 Navistar MaxxForce 13 six-cylinder heavy-duty diesel engine modified to reach peak thermal efficiency, as per the goals of the SuperTruck program. A schematic of the test engine configuration is shown in Figure 1, along with basic engine specifications in Table 1.

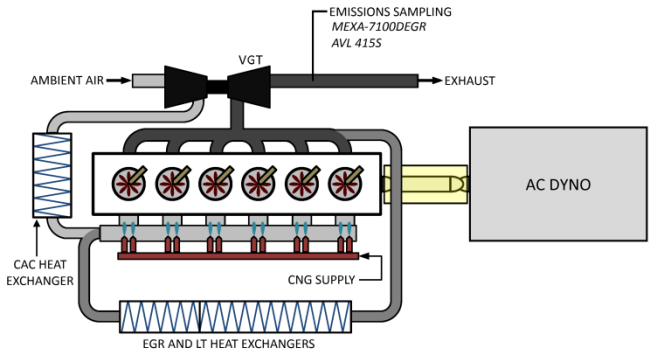

Figure 1 Schematic of test engine configuration

The SuperTruck engine features an air system configured for high thermal efficiency, utilizing a single stage turbocharger and a dual-pass EGR cooler with high and low temperature stages. Prototype pistons feature a higher than stock compression ratio. A 2500 bar capable common-rail diesel fuel injection system is used with prototype injectors.

Table 1 Engine Specifications

	Navistar 13L DF
CYLINDERS[-]	6
BORE [mm]	126
STROKE [mm]	166
DISPLACEMENT [L]	12.4
CR[-]	>17
DI PRESS. [bar]	2500
PFI PRESS. [bar]	6

Several alterations to the production engine were made to enable and enhance low-temperature dual-fuel combustion. A prototype variable geometry turbine (VGT) turbocharger was implemented to decrease pumping losses compared to the OEM two stage system. A modified intake manifold is used which incorporates two port fuel injection (PFI) injectors per cylinder. The natural gas fuel is injected at 6 bar above intake manifold pressure directed at the intake runner of each cylinder.

Stock EGR cooling systems are maintained. A building process water system is used for cooling heat exchangers in the high and low temperature engine coolant loops, and to directly cool the high pressure charge air cooler. Cooling systems were tuned using Navistar internal metrics to mimic heat rejection available in a production vehicle. Intake and exhaust restrictions were likewise adjusted to simulate vehicle air filtration systems along with exhaust aftertreatment and muffler restrictions. Constant restrictions were used across all tested conditions. Start of injection timing, both as a reported value and used in computation of ignition delay, is determined from the engine control unit command and not directly measured from injector current.

Test Fuels

The dual-fuel operating strategy employed in this study uses two fuels concurrently: a low-reactivity fuel (natural gas) along with a high-reactivity fuel (diesel). Natural gas was chosen to provide a high resistance to autoignition and has been used as a low reactivity fuel by [18,19] to increase the full load capability for RCCI combustion. The natural gas used in this study was supplied by pipeline, while the diesel fuel was an ultra-low sulfur (ULSD) certification fuel. The natural gas constituents were analyzed on-site using a gas chromatograph. Relevant properties of the natural gas and diesel fuels are listed in Table 2.

Table 2 Fuel Properties

	Natural Gas		**Diesel**
DENSITY [KG/M³]	0.724	***DENSITY [KG/L]***	0.851
NET HV [MJ/KG]	47.47	***NET HV [MJ/KG]***	42.8
MN [-]	95.17[1]	***CN [-]***	44
MON [-]	131.95	***AROMATICS [%]***	28
CN [-]	-	***OLEFINS [%]***	1
METHANE [MOL/MOL]	0.931	***SATURATES [%]***	71
ETHANE [MOL/MOL]	0.0459	***H:C RATIO [-]***	1.88
PROPANE [MOL/MOL]	0.00183	***SULFUR [PPM]***	10
NITROGEN [MOL/MOL]	0.0085	***T_{10} [°C]***	214
CO_2 [MOL/MOL]	0.01145	***T_{50} [°C]***	259
H:C RATIO [-]	3.90	***T_{90} [°C]***	317

Operating Conditions and Limits

To constrain the results to more realistic operating conditions, limits were placed on the emissions and engine operation. Peak cylinder pressure (PCP) is limited to 250 bar, while maximum rate of pressure rise (for each cylinder, measured on an unfiltered cylinder pressure signal) is limited to less than 15 bar/deg. Combustion noise was targeted to be less than 92 dBa. This target is established as an outer boundary based on guidelines from the USCAR Advanced Combustion & Emissions Control (ACEC) working group [21].

Engine-out NO_x emissions targets for this work have been relaxed compared to past RCCI results because maximum brake thermal efficiency (BTE) is one goal for the SuperTruck project. When not using EGR, NO_x emissions were targeted to be less than 10 g/kW-hr, and with EGR NO_x was targeted to be roughly half of that while minimizing the BTE penalty for the lowest minimal total fluid consumption. The 10 g/kWh NO_x target was chosen based on the assumption of the use of a selective catalytic reduction (SCR) aftertreatment system with 98% conversion efficiency in order to meet EPA 2010 emissions standards for heavy-duty on-road engines

Soot emissions are not explicitly limited, but were kept below 1 filter smoke number (FSN). Likewise, explicit limits are not placed on CO or HC emissions, but were typically minimized to increase thermal efficiency. Combustion stability was maintained at each operating point, with a COV of engine-averaged IMEP less than 2% for all tested conditions.

Procedure

The engine was operated at steady-state conditions representative of the EPA 13 mode supplemental emissions test (SET) to get cycle averaged quantities of emissions and efficiency using the mandated weighting factors [22].

The engine was operated to have a simulated engine power curve with a peak load of 20 bar BMEP and peak rated power of 312 kW.

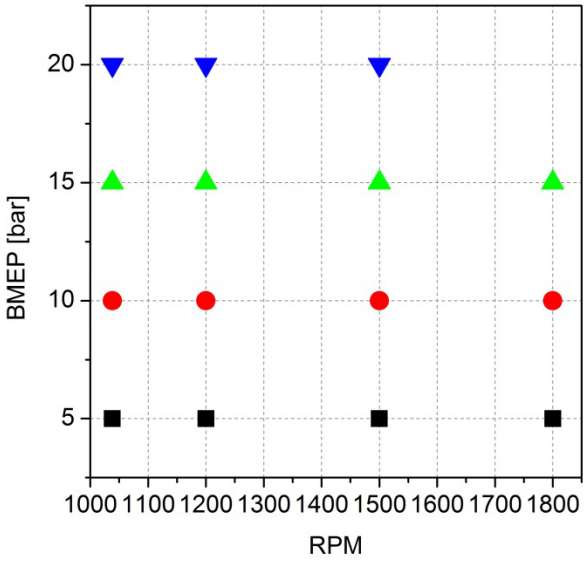

Figure 2 Engine speed and load tests points representative of the EPA 13 mode SET

The test points were chosen to have the ability to simulate a down speeded or standard speed power curve to examine the effect of the engine speed on the cycle averaged NO_x emissions. A speed was defined as 1038, B speed was 1200 and C speed was 1500 rpm for a simulated down-speeded engine while A, B and C speeds for the standard speed engine were 1200, 1500 and 1800 rpm, respectively.

[1] Methane Number (MN) and MON calculated from [20]

Definitions and Efficiencies

Different definitions of efficiencies and emissions values are included in the paper in addition to the standard brake specific emissions and efficiency values.

Both engine-out and simulated tailpipe-out emissions will be discussed. Engine-out emissions are directly measured by the emissions bench, while tailpipe-out emissions are simulated by applying aftertreatment efficiency values to the engine-out emissions.

From the brake specific emissions values (both engine-out and tailpipe-out) measured at each of the 13 modes, the cycle averaged emissions and efficiency values was also calculated from the 13 mode test weighting factors. Additionally, since the paper assumes the use of a urea SCR system for NO_x control, the amount of urea usage is estimated. Using a similar method as Kokjohn [23], the cycle averaged NO_x result multiplied by an SCR efficiency (98% in this case). Next, that value is then multiplied by a 1% urea per g/kWh NO_x factor from [23] to get the urea usage. Finally, since urea is currently similar in price to ULSD, urea usage (and heating value) is simulated to be equal to that of ULSD. Adding the total fuel consumption (ULSD+CNG) to the urea usage, the total fluid consumption can be calculated. From this total fluid consumption, a total fluid equivalent BTE can be calculated by dividing the brake power by the total fluid consumption energy.

RCCI Operating Strategy

To achieve dual fuel combustion, the low-reactivity natural gas was introduced via port injection and the high-reactivity diesel fuel was introduced via direct injection into the cylinder during the compression stroke. A schematic of typical port and direct injection timings is included in Figure 3.

The single natural gas port fuel injection used a constant start of injection timing of -570°ATDC for all test cases. Single and double pulses were used for the diesel injection, with the pilot injection phased early in the compression stroke (-55°ATDC) and the main injection near top dead center (-10 to 15°ATDC). Typical pilot mass fractions ranged from 5 to 10% of the total DI fuel.

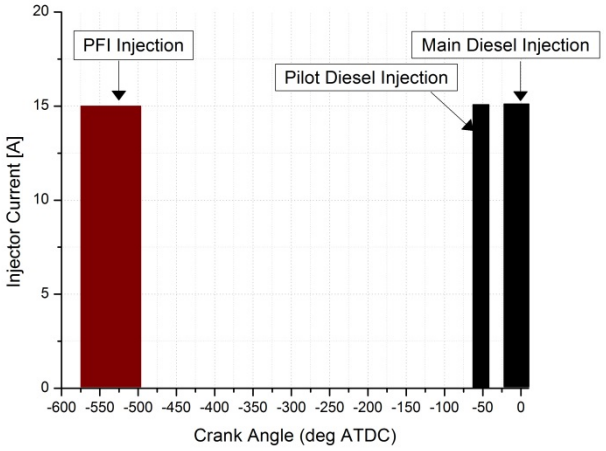

Figure 3 Representative injection strategy with PFI injection during intake stroke and the dual direct diesel injections

Again, this strategy differs from past, fully premixed results and more closely follows [13-17], which were designed to reach high loads while keeping noise and peak cylinder pressure within acceptable limits. The late diesel injection also offers increased control of the combustion phasing using SOI timing.

The engine operating strategy was derived from work by Wissink [17] and used in [24]. Based on results from [24], the same operating strategy was used to operate the engine at higher speeds. Figure 4 shows the cylinder pressure and AHRR for cylinder 2.

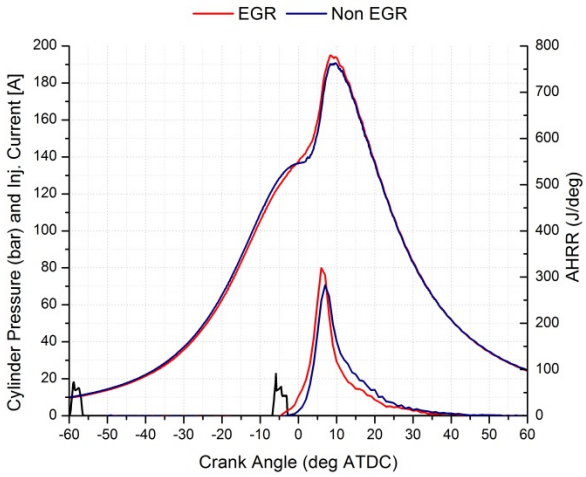

Figure 4 Representative operating conditions with and without EGR showing the cylinder pressure, injection current and apparent heat release rate

Table 3 gives representative operating parameters operating conditions with and without EGR. Overall, it can be seen that there were slight changes to the main SOI timing, PFI fraction, intake temperature and rail pressure between EGR operation.

Table 3 Representative Operating Condition Parameters

	EGR	Non-EGR
BMEP [BAR]	15	15
SPEED [RPM]	1200	1200
EGR [%]	8	0
P_{INT} [BAR]	2.18	2.18
T_{INT} [°C]	49.2	46.1
PFI MASS FRACTION [%]	47.7	48.4
RAIL PRESSURE [BAR]	700	500
PILOT/MAIN SOI [°ATDC]	-68/-4	-68/-8
CA_{50} [DEG ATDC]	10.1	8.6
MPRR [BAR/DEG]	12	15
COMB. NOISE [DBA]	87	89

Results

EGR

The engine was operated both without EGR and with low levels of EGR in RCCI combustion mode over the 13 modes. When using EGR, the goal was to reach the maximum NO_x reduction for the minimal BTE loss. The result was a lower amount of EGR compared with previous RCCI results (<50%) [6]. Figure 5 shows the amount of EGR decreased with load to minimize PMEP and soot emissions, similar results in [6].

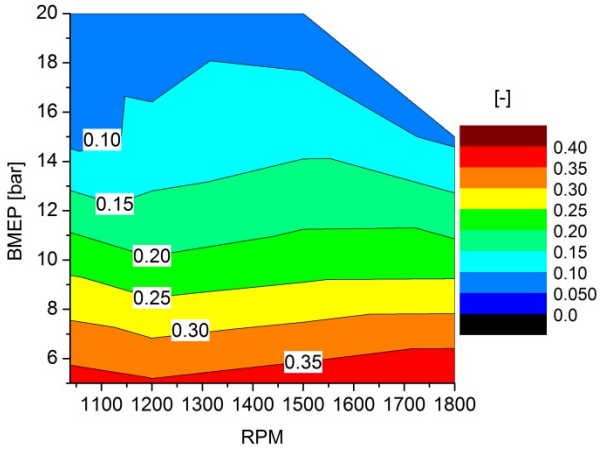

Figure 5 EGR percentage over the full engine operating map

While these EGR quantities match well with the current turbocharger, compression ratio, combustion targets, injector and piston bowl shape, higher amounts of EGR could be used with different hardware depending on the goals for BTE, NO_x and soot.

PFI Mass Fraction

Similar to previous RCCI results, the PFI mass fraction varies with speed and load to optimize the combustion phasing. Figure 7 and Figure 6 shows there were similar PFI mass fractions between both conditions. However, a higher PFI mass fraction was used without EGR at loads below 12.5 bar BMEP and speeds less than 1500 rpm to keep the MPRR below 15 bar/deg.

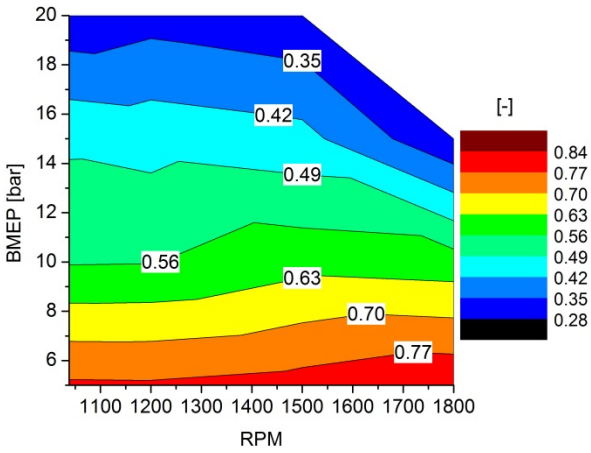

Figure 6 PFI mass fraction for EGR operation over the full engine operating map

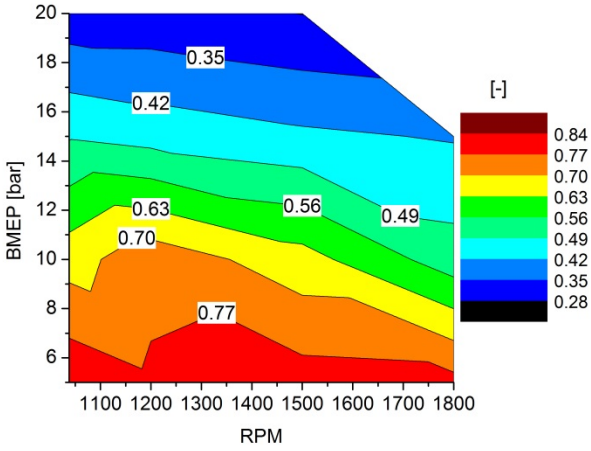

Figure 7 PFI mass fraction for non-EGR operation over the full engine operating map

In contrast to previous fully premixed RCCI results where the highest PFI mass fraction was found at high loads, the new operating strategy limits the PFI mass fraction at high loads to control combustion noise [24]. Lower compression ratio could help to increase the PFI mass fraction at high loads and decrease it at low loads, depending on which type of port fuel is used.

NO_x

Figure 8, shows the NO_x with EGR. Peak less than the 10 g/kWh target by almost a factor of 2. NO_x was much lower at higher engine speeds due to the reduced residence time.

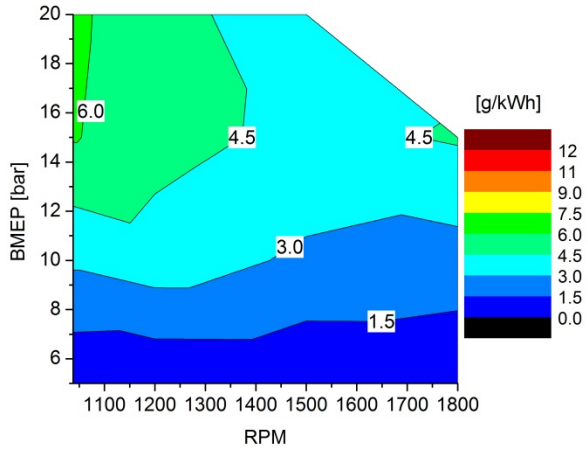

Figure 8 NO_x emissions for EGR operation over the full engine operating map

In Figure 9, the max NO_x without EGR was slightly over the 10 g/kWh target at high load and low speed. NO_x without EGR was also lower at higher engine speeds.

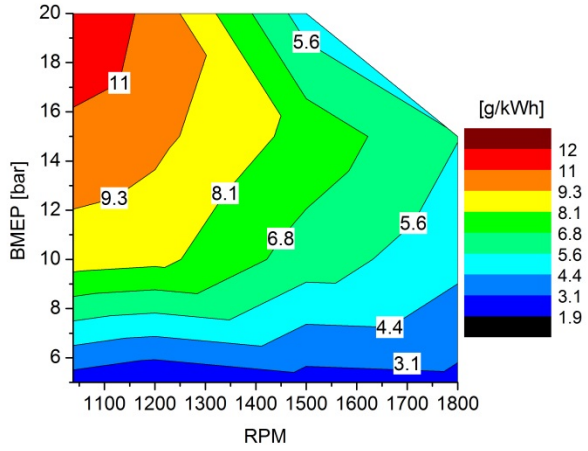

Figure 9 NO_x emissions for non-EGR operation over the full engine operating map

This NO_x reduction with engine speed could be useful in the design of the engine power curve. Depending on the BTE, a low NO_x, high-speed calibration could be used vs a high NO_x, low-speed calibration. However, for this engine map, the cycle-averaged BTE going from the higher NO_x, down-speed calibration to the standard speed calibration decreases less than the improvement in total fluid consumption. The cycle-averaged BTE dropped by 1% while the fuel saved from lower urea usage only increased the total fluid consumption BTE by 0.5%, indicating a net loss of total fluid consumption BTE of 0.5%.

Figure 8 shows that when using EGR, the engine-out cycle-averaged NO_x was reduced by 48% from 8.1 to 4.2 g/kWh using the down-speed power curve. The standard-speed power curve with EGR lowered NO_x by 41% from 6.4 to 3.75 g/kWh.

For tailpipe out emissions, it was assumed that a 98% efficient selective catalytic reduction (SCR) system would be used. The tail pipe-out, cycle-averaged NO_x for the down-speed case was similarly reduced by 48% from 0.16 to 0.084 g/kWh. The standard speed tail pipe-out NO_x was reduced 41% from 0.128 to 0.0746 g/kWh. Both of these results are lower than the EPA2010 NO_x standard level of 0.27 g/kWh.

Soot

There were low engine–out soot emissions for both strategies. The low soot was due to the late main injection and high compression ratio where high combustion temperatures and the premixed natural gas limit soot emissions.

Next, since it has been shown that FSN to particulate mass correlations may not be not accurate for RCCI combustion, only FSN values will be given [24].

Figure 10 shows that the soot slightly increased with load and speed due to the lower PFI mass fraction and increased amount of late fuel injection.

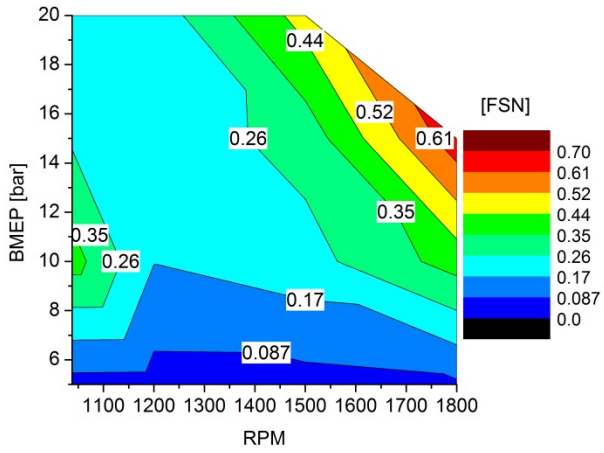

Figure 10 Soot emissisons for EGR operation over the full engine operating map

There was a slight overall decrease in soot when not using EGR, as shown in Figure 11. As with CDC, the use of a late main injection displays the classic soot/NO_x tradeoff behavior when combustion temperatures and oxygen concentration drop with EGR.

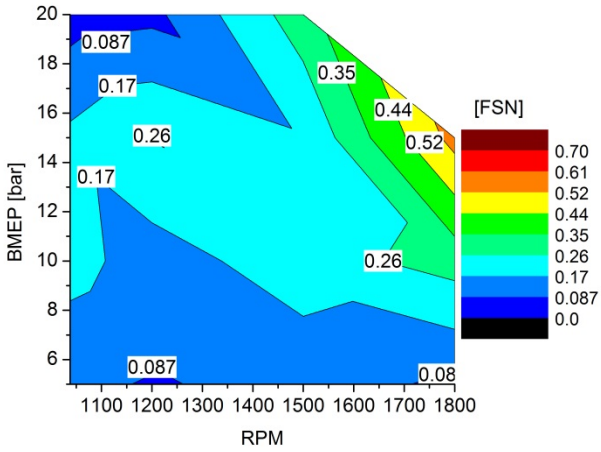

Figure 11 Soot emissions for non-EGR operation over the full engine operating map

The highest soot emissions for both cases were seen at high speed and high load. Similar to CDC, there was less time available for fuel-air mixing and a reduced PFI mass fraction.

The cycle-averaged soot was 0.18 FSN with EGR and 0.13 FSN without EGR. When simulating the use of a 98% effective DPF, the tailpipe out soot was 0.0036 FSN with EGR vs 0.0026 without.

HC

Similar to other RCCI results, HC emissions are higher than with CDC. Figure 12 shows the HC emissions follow very closely to the PFI mass fraction, indicating that the HC was likely unburned port injected fuel escaping combustion.

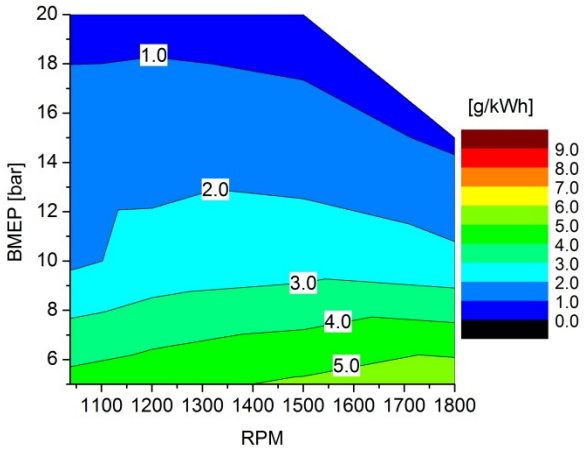

Figure 12 HC emissisons for EGR operation over the full engine operating map

HC emissions without EGR are increased due to the higher exhaust mass flow rate out of the engine; with the HC not having an extra chance for complete oxidation, as shown in Figure 13. Engine-out HC emissions for the EGR case was 1.526 g/kWh vs 2.27 g/kWh for the non-EGR case.

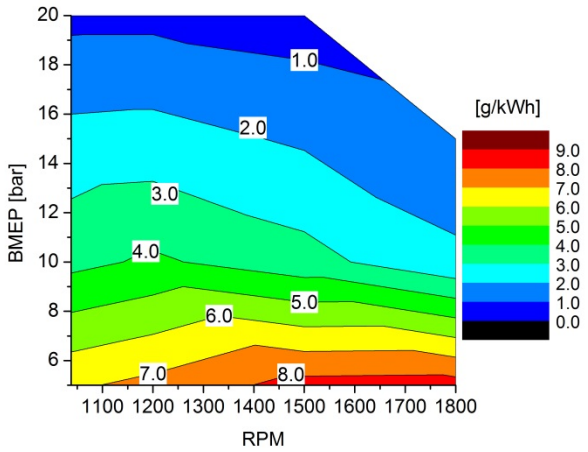

Figure 13 HC emissions for non-EGR operation over the full engine operating map

CH_4

Since the port fuel was natural gas, the CH_4 emissions for the tests were high. Comparing Figure 12 and Figure 13 to Figure 14 and Figure 15, the CH_4/THC fraction was 0.6-0.8 for most data points, as also seen in [24].

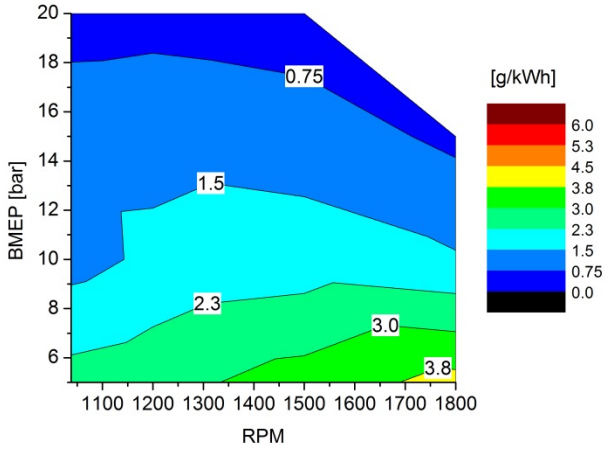

Figure 14 CH_4 emssions EGR operation over the full engine operating map

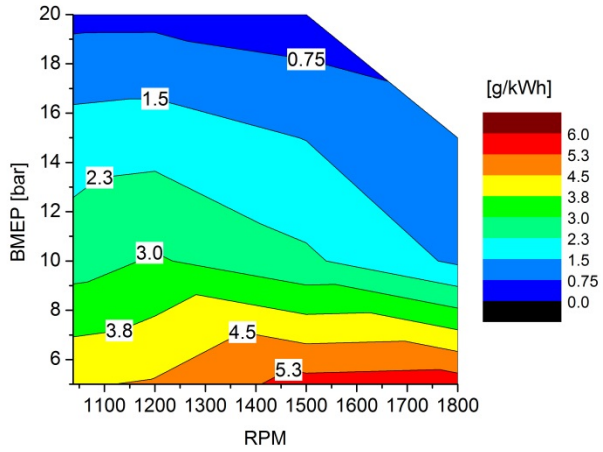

Figure 15 CH_4 emissions for non-EGR operation over the full engine operating map

With the high fraction of CH_4 in the total HC, the non-methane HC are low and should be able to be treated with an oxidation catalyst, as the exhaust gas temperatures were 300 to 500°C [25].

However, the rest of the HC are CH_4, they could be difficult to oxidize at these exhaust temperatures so there is more work needed to reduce CH_4 emissions.

CO

Figure 16 shows that the CO emissions also follow past RCCI trends, where they were higher at low loads and temperatures with or without EGR.

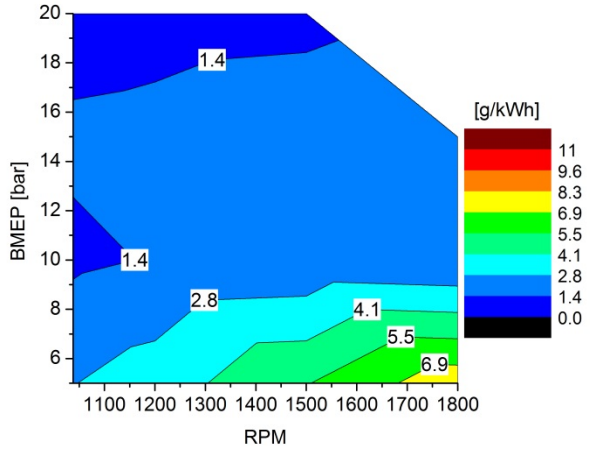

Figure 16 CO emissions for EGR operation over the full engine operating map

Similar to HC, CO was also higher without EGR, as the CO was not recycled in additional engine cycles and due to the higher intake temperature seen when using EGR, as shown in Figure 17.

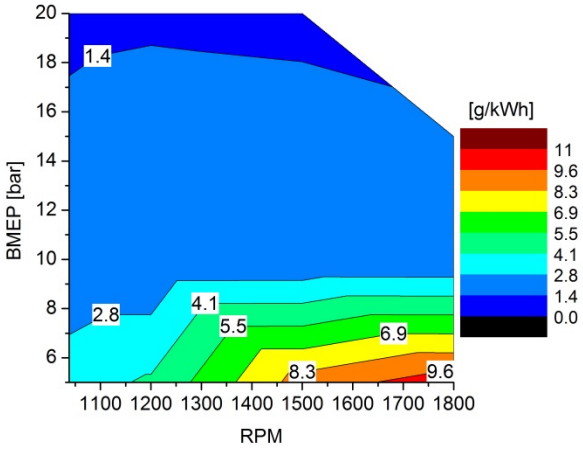

Figure 17 CO emissions for non-EGR operation over the full engine operating map

Engine-out CO with EGR was 1.538 g/kWh vs 1.78 g/kWh for the non-EGR case. CO can be treated at the present exhaust conditions with an oxidation catalyst [25].

Combustion Noise

By letting the NO_x emissions increase above the EPA2010 standard levels, it was hoped to be able to reduce the MPRR and combustion noise compared to previous fully premixed RCCI strategies. The next section looks at typical metrics for noise such as MPRR, ringing intensity and combustion noise.

Maximum Pressure Rise Rate

Maximum pressure rise rate has been used as a method for quantifying combustion noise between different engines, labs, etc. Figure 18 shows the 15 bar/deg target was reached except at the 1800 rpm, 15 bar BMEP non EGR point. Typically, 10 bar/deg has been used as a target, but because of the high compression ratio, the motored MPRR is higher than typically seen and the 15 bar/deg target was used. Note that the engine was operated with the MPRR limit first, letting the combustion noise and ringing intensity float, sometimes above the guideline values.

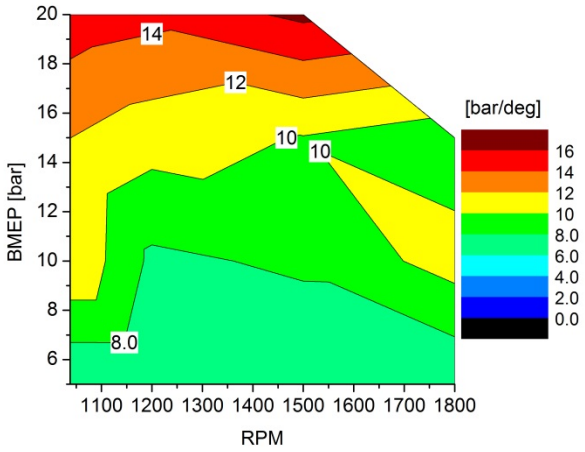

Figure 18 MPRR for EGR operation over the full engine operating map

Figure 19 shows that EGR reduced MPRR over a wide area of the map due to later CA50. Interesting to note that MPRR doesn't always correlate to noise, this is especially evident at 20 bar BMEP from 1038 to 1500 rpm where the MPRR is constant and the combustion noise increases from 88 to 93 dBa.

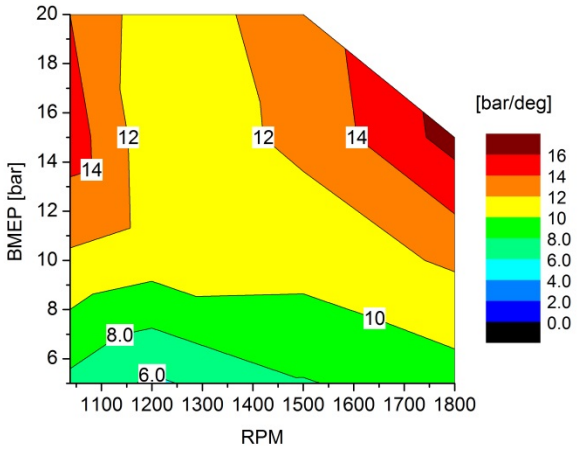

Figure 19 MPRR for non-EGR operation over the full engine operating map

Ringing Intensity

Ringing intensity can be used as an alternative methodology to provide a more qualitative metric for combustion noise than MPRR by calculating the acoustic energy from the combustion event. In this work, the ringing intensity guideline, which we are comparing our result with, was 5 MW/m^2 [28]. In Figure 20, EGR reduced ringing intensity due to later CA50 timing compared to Figure 21. With EGR, ringing intensity at 1800 rpm, 15 bar BMEP was reduced (over Figure 21) due to the lower PFI mass fraction compared to EGR operation.

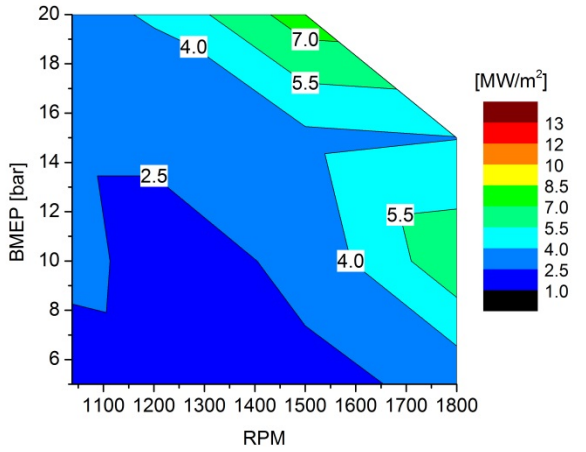

Figure 20 Ringing intensity for EGR operation over the full engine operating map

However, with EGR, 1800 rpm, 10 bar BMEP and 1500 rpm, 20 bar BMEP slipped above 5 MW/m^2 even though the MPRR was less than15 bar/deg. Without EGR, the ringing intensity was above 5 MW/m^2 at 1800 rpm for all loads.

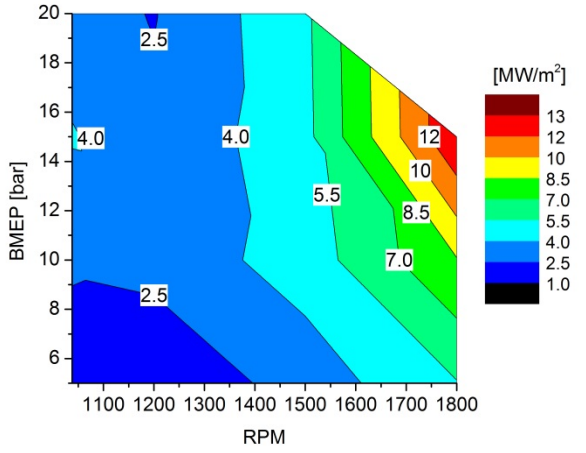

Figure 21 Ringing intensity for non-EGR operation over the full engine operating map

Fine tuning to the PFI mass fraction should bring down the ringing intensity below 5 MW/m^2 everywhere in the operating map, but at the expense of possible decreased thermal efficiency.

Combustion Noise

Next, combustion noise was calculated using the AVL software. Guidelines from the USCAR advanced engine and combustion (ACEC) team for combustion noise for light-duty vehicles were used as the results compared against [21] with a maximum of ~92 dba at full speed and load although heavy-duty noise targets could be higher depending on OEM

standards. Figure 22 shows that with EGR, the results were close to the guideline of 92 dBa, with a progression towards increased noise at high speed and load.

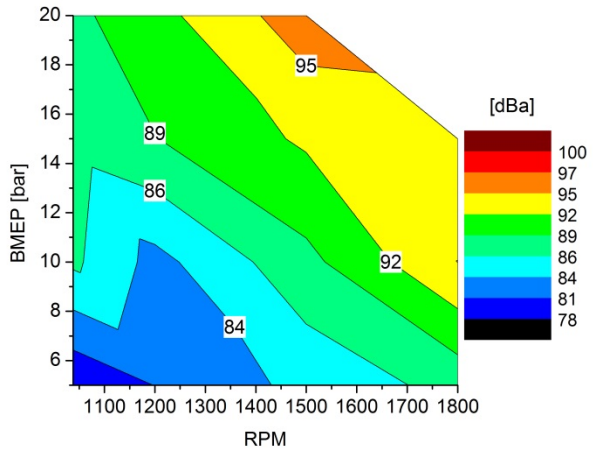

Figure 22 Combustion noise for EGR operation over the full engine operating map

Without EGR, the combustion noise was below the guidelines except at the 1800 rpm 15 bar condition, as shown in Figure 23. Again, fine tuning with PFI mass fraction could lower the high speed, high-load noise to the 92 dBa target.

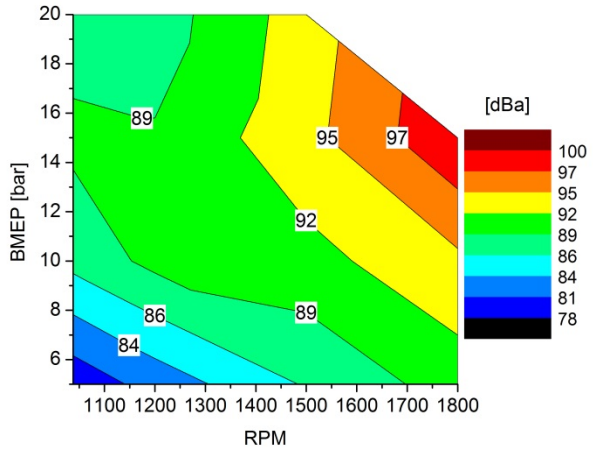

Figure 23 Combustion noise for non-EGR operation over the full engine operating map

Overall, combustion noise metrics increased with load due to the increased injected quantity of fuel and maximum heat release rate. Combustion noise metrics also increased with engine speed even though the MPRR was less than 15 bar/deg. As engine speed increases, the time for each combustion cycle reduces, making the pressure rise rate as a function of time (i.e. dp/dt, instead of dp/dCA) increase. This more rapid combustion increases noise.

Brake Thermal Efficiency

Finally, another goal of the paper was to find the maximum BTE without EGR and the maximum BTE with lower NO_x with the least BTE penalty.

When using EGR, the peak BTE was 46.5% at 1038 rpm, 15 bar BMEP, however the cycle averaged BTE is 43.5%, as shown in Figure 24

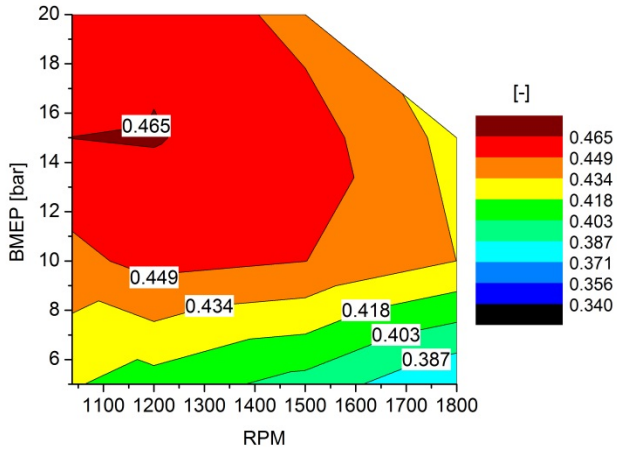

Figure 24 Brake thermal efficiency for EGR operation over the full engine operating map

In Figure 25, the maximum BTE was 46.8% at 1038 rpm and 20 bar BMEP, with a cycle averaged BTE of 43.7%. Like most other engines the BTE peak occurs near the rated torque speed, at high-load condition. This is because of the low PMEP and friction.

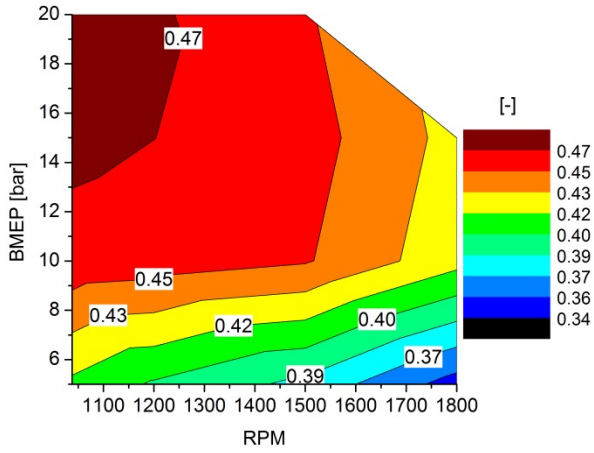

Figure 25 Brake thermal efficiecny for non-EGR operation over the full engine operating map

The reason for the difference in the cycle averaged values compared to the difference in the peak values is the

undersized turbocharger. There was less pumping work at high speeds when diverting some of the flow to the EGR system. With an optimally sized turbocharger for the overall engine cycle, the non-EGR case would likely have higher cycle averaged BTE than the EGR case.

Discussion

A dual-fuel, low temperature combustion strategy was used to achieve high BTE with low combustion noise at the expense of increased NO_x emissions. While high BTE is always desired; depending on the engine-out NO_x emissions, the total fluid consumption might not be minimum at max BTE. Thus, one needs to determine the optimal BTE/NO_x/urea tradeoff for the lowest total fluid consumption, when equipped with a urea SCR system for NO_x abatement.

Figure 26 compares the results (black circles) to a heavy-duty diesel baseline engine (blue square) with 45% BTE and 4 g/kWh NO_x and 1.3% BTE loss from urea consumption for total fluid consumption BTE of 43.7%.

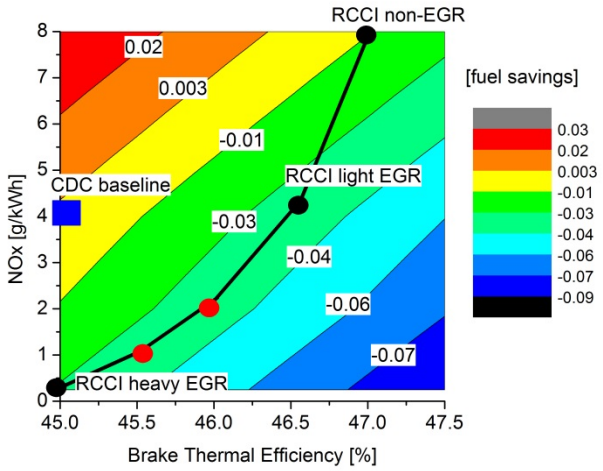

Figure 26 Comparison of RCCI and CDC operating points for fuel consumption savings against the CDC baseline. Blue square is the CDC baseline. Black circles are RCCI cases without EGR, light EGR and heavy EGR. Red circles are simulated RCCI points with EGR.

The contour values for fuel savings represent the total fluid consumption reduction for various RCCI NOx and BTE combinations relative to the CDC 45% value.

The black circles were measured points of the 8 g/kWh non-EGR NO_x case, the 4 g/kWh light EGR case and a previous low NO_x, high EGR RCCI case [8]. The red dots are simulated points where the 2x NO_x reduction per 0.5 point drop in BTE is continued. If these points are possible, then a 2 g/kWh NO_x calibration would yield a slightly improved total fluid consumption compared to the measured 4 g/kWh results. Similar values for low total fluid consumption were shown in [29]. Here the lowest total fluid consumption using EGR for CDC was between 3-4 g/kWh, when urea and fuel were assumed to be the same price.

Conclusions

The full engine operating map of a heavy-duty diesel engine using RCCI combustion was investigated using natural gas and ULSD fuels. Using a previously developed RCCI engine operating strategy [24], the whole engine operating map was explored with and without EGR. From the results of these tests, the following conclusions are drawn:

The cycle averaged NO_x emissions were 8 g/kWh without EGR. The relaxed NO_x targets allowed for lower combustion noise (< 100 dBa) and higher loads (up to 20 bar BMEP) than previous RCCI studies.

RCCI operation with EGR showed to have the lowest total fluid consumption due to the use of an SCR. A model shows it might be possible to further decrease the total fluid consumption by going to engine out, cycle averaged 2 g/kWh NO_x.

References

1. “Greenhouse Gas Emissions Standards and Fuel Efficiency Standards for Medium- and Heavy-Duty Engines and Vehicles,” Federal Register 76(179): 57106-57513, 2011.
2. “Control of Air Pollution from New Motor Vehicles: Heavy-Duty Engine and Vehicle Standards and Highway Diesel Fuel Sulfur Control Requirements,” Federal Register 66(12): 5002-5193, 2001.
3. "Recovery Act—Systems Level Technology Development, Integration, and Demonstration for Efficient Class 8 Trucks (SuperTruck) and Advanced Technology Powertrains for Light Duty Vehicles (ATP-LD)," DE-FOA-0000079, Department of Energy: Washington, D.C., 2009.
4. De Ojeda, W. and Rajkumar, M., "Engine Technologies for Clean and High Efficiency Heavy Duty Engines," *SAE Int. J. Engines* 5(4):1759-1767, 2012, doi:10.4271/2012-01-1976.
5. Kokjohn, S., Hanson, R., Splitter, D., and Reitz, R., "Experiments and Modeling of Dual-fuel HCCI and PCCI Combustion Using In-Cylinder Fuel Blending," *SAE Int. J. Engines* 2(2):24-39, 2010, doi:10.4271/2009-01-2647.
6. Hanson, R., Kokjohn, S., Splitter, D., and Reitz, R., "An Experimental Investigation of Fuel Reactivity Controlled PCCI Combustion in a Heavy-Duty Engine," *SAE Int. J. Engines* 3(1):700-716, 2010, doi:10.4271/2010-01-0864.
7. Joo, S., Alger, T., Chadwell, C., De Ojeda, W. et al., "A High Efficiency, Dilute Gasoline Engine for the Heavy-Duty Market," *SAE Int. J. Engines* 5(4):1768-1789, 2012, doi:10.4271/2012-01-1979.
8. Zhang, Y., Sagalovich, I., De Ojeda, W., Ickes, A. et al., "Development of Dual-Fuel Low Temperature Combustion Strategy in a Multi-Cylinder Heavy-Duty Compression Ignition Engine Using Conventional and

Alternative Fuels," *SAE Int. J. Engines* 6(3):1481-1489, 2013, doi:10.4271/2013-01-2422.
9. Ickes, A., Wallner, T., Zhang, Y., and De Ojeda, W., "Impact of Cetane Number on Combustion of a Gasoline-Diesel Dual-Fuel Heavy-Duty Multi-Cylinder Engine," *SAE Int. J. Engines* 7(2):860-872, 2014, doi:10.4271/2014-01-1309.
10. Teetz, C., Bergmann, D., Schneemann, A., et al., "MTU HCCI Engine with Low Raw Emissions," *MTZ* 73(9):4-9, 2012.
11. De Ojeda, W., Zhang, Y., Xie, K., Han, X. et al., "Exhaust Hydrocarbon Speciation from a Single-Cylinder Compression Ignition Engine Operating with In-Cylinder Blending of Gasoline and Diesel Fuels," SAE Technical Paper 2012-01-0683, 2012, doi:10.4271/2012-01-0683.
12. Zhang, Y., De Ojeda, W., and Wickman, D., "Computational Study of Combustion Optimization in a Heavy-Duty Diesel Engine Using In-Cylinder Blending of Gasoline and Diesel Fuels," SAE Technical Paper 2012-01-1977, 2012, doi:10.4271/2012-01-1977.
13. Sun, Y. and Reitz, R., "Adaptive Injection Strategies (AIS) for Ultra-Low Emissions Diesel Engines," SAE Technical Paper 2008-01-0058, 2008, doi:10.4271/2008-01-0058.
14. Sun, Y. and Reitz, R., "Modeling Diesel Engine NOx and Soot Reduction with Optimized Two-Stage Combustion," SAE Technical Paper 2006-01-0027, 2006, doi:10.4271/2006-01-0027.
15. Kokjohn, S. and Reitz, R., "A Computational Investigation of Two-Stage Combustion in a Light-Duty Engine," *SAE Int. J. Engines* 1(1):1083-1104, 2009, doi:10.4271/2008-01-2412.
16. Weninger, E., “MS Thesis in Progress”, University of Wisconsin-Madison, 2015.
17. Wissink, M. and Reitz, R., "Direct Dual Fuel Stratification, a Path to Combine the Benefits of RCCI and PPC," *SAE Int. J. Engines* 8(2):878-889, 2015, doi:10.4271/2015-01-0856.
18. Walker, N. R., Wissink, M. L., DelVescovo, D. A., and Reitz, R. D., "Use of Natural Gas for Load Extension of Dual-Fuel Reactivity Controlled Compression Ignition Heavy-Duty Engine Operation", Journal of Energy Resources Technology, 2015, JERT-15-1031, doi:10.1115/1.4030110
19. Nieman, D., Dempsey, A., and Reitz, R., "Heavy-Duty RCCI Operation Using Natural Gas and Diesel," *SAE Int. J. Engines* 5(2):270-285, 2012, doi:10.4271/2012-01-0379.
20. “Methane Number and Fuel Composition.” California Air Resources Board, 21 Feb. 2002. Web. 03 Apr. 2014.
21. USCAR Advanced Combustion & Emissions Control working group combustion noise standards for light-duty engines. 2015.
22. 40 CFR Ch.1, 86.1360-2007, Supplemental emission test; test cycle and procedures.
23. Kokjohn, S., “Reactivity Controlled Compression Ignition Combustion”, PhD dissertation, Department of Mechanical Engineering, University of Wisconsin-Madison, 2012.
24. Hanson, R., Ickes, A., and Wallner, T., “Use of Adaptive Injection Strategies to Increase the Full Load Limit of RCCI Operation”, Proceedings of the ASME ICEF conference, ICEF2015-1115. 2015.
25. Khalek, T., et al., “Phast 1 of the Advanced Collaborative Emissions strudy (ACES): Highighlights of Project Finding” US DOE DEER Conference, Dearborn MI, 2009
26. Prikhodko, V., Curran, S., Barone, T., Lewis, S. et al., "Emission Characteristics of a Diesel Engine Operating with In-Cylinder Gasoline and Diesel Fuel Blending," *SAE Int. J. Fuels Lubr.* 3(2):946-955, 2010, doi:10.4271/2010-01-2266.
27. Johnson, T., “Diesel Emissions in Review,” *SAE Int. J. Engines*, 4(1):143-157, 2011, doi:10.4271/2011-01-0304.
28. Eng, J., "Characterization of Pressure Waves in HCCI Combustion," SAE Technical Paper 2002-01-2859, 2002, doi:10.4271/2002-01-2859.
29. Winsor, R., et al., “Efficiency and Emission Improvements for Future Off-road Engines”, ERC Symposium, Madison, Wisconsin, 2015.

Acknowledgments

This study was supported by the U.S. Department of Energy (DOE), the National Energy Technology (NETL) office, under cooperative agreement “SuperTruck – Development and Demonstration of a Fuel-Efficient Class 8 Tractor & Trailer” DOE Contract: DE-EE0003303. The authors wish to thank Roland Gravel, Gurpreet Singh, and Ken Howden of DOE and Ralph Nine of NETL for their continuing support.

Additionally, the authors would like to acknowledge Navistar for their continued partnership in this work thru the SuperTruck program, and acknowledge Jim Cigler, James Park, and Gengxin Han for technical support and discussions.

Crank-angle resolved data processing, including calculation of heat release, was performed using AVL Concerto. The authors wish to express their gratitude to staff at AVL North America Inc. for their support.

publicly and display publicly, by or on behalf of the Government.

Definitions/Abbreviations

ACEC	Advanced Combustion & Emissions Control
AFR	Air Fuel Ratio
AHRR	Apparent Heat Release Rate
AIS	Adaptive Injection Strategies
AKI	Anti Knock Index
ATDC	After Top Dead Center
BMEP	Brake Mean Effective Pressure
BTE	Brake Thermal Efficiency
CA	Crank Angle
CDC	Conventional Diesel Combustion
CN	Cetane Number
CO	Carbon Monoxide
COV	Coefficient of Variation
DDFS	Dual Direct Fuel Stratification
DI	Direct-Injection
DOE	Department of Energy
DPF	Diesel Particulate Filter
EGR	Exhaust Gas Recirculation
EGT	Exhaust Gas Temperature
EPA	Environmental Protection Agency
FID	Flame Ionizing Detector
FSN	Filter Smoke Number
FTE	Friction Thermal Efficiency
HC	Hydrocarbon
HCCI	Homogeneous Charge Compression Ignition
HRR	Heat Release Rate
IMEP	Indicated Mean Effective Pressure
LHV	Lower Heating Value
LTC	Low Temperature Combustion
MAF	Mass Air Flow
MON	Motor Octane Number
MHRR	Maximum Heat Release Rate
MN	Methane Number
MPRR	Maximum Pressure Rise Rate
NMEP	Net Mean Effective Pressure
NMHC	Non Methane Hydrocarbons
NO_x	Oxides of Nitrogen
NTE	Net Thermal Efficiency
OEM	Original Equipment Manufacturer
PCP	Peak Cylinder Pressure
PFI	Port-Fuel-Injection
PHI	Equivalence Ratio
PM	Particulate Matter
PMEP	Pumping Mean Effective Pressure
PON	Pump Octane Number
PPM	Parts Per Million
PRR	Pressure Rise Rate
PTE	Pumping Thermal Efficiency
RCCI	Reactivity Controlled Compression Ignition
RON	Research Octane Number
SCR	Selective Catalytic Reduction
SI	Spark Ignition
SOI	Start of Injection
TDC	Top Dead Center
ULSD	Ultra Low Sulfur Diesel
US	United States
VGT	Variable Geometry Turbine